Two relaxation mechanisms observed in transport between spin-split edge states at high imbalance

E. V. Deviatov,[1,*] A. Würtz,[2] A. Lorke,[2] M. Yu. Melnikov,[1] V. T. Dolgopolov,[1] D. Reuter,[3] and A. D. Wieck[3]
[1]*Institute of Solid State Physics RAS, Chernogolovka, Moscow District 142432, Russia*
[2]*Laboratorium für Festkörperphysik, Universität Duisburg-Essen, Lotharstrasse 1, D-47048 Duisburg, Germany*
[3]*Lehrstuhl für Angewandte Festkörperphysik, Ruhr-Universität Bochum, Universitätsstrasse 150, D-44780 Bochum, Germany*
(Received 24 March 2003; published 24 March 2004)

Using a quasi-Corbino geometry to directly study electron transport between spin-split edge states under high imbalance conditions, we find a pronounced hysteresis in the *I-V* curves originating from dynamic nuclear polarization near the sample edge. Already in the simplest case of filling factor $\nu=2$ we observe a complicated relaxation, depending on the sign of the electrochemical potential difference. The characteristic relaxation times are about 25 s and 200 s, which points to the presence of two different relaxation mechanisms. The two time constants are ascribed to the formation of a local nuclear polarization due to flip-flop processes and the diffusion of nuclear spins.

DOI: 10.1103/PhysRevB.69.115330 PACS number(s): 73.40.Qv, 71.30.+h

I. INTRODUCTION

In a quantizing magnetic field, energy levels in a two-dimensional electron gas (2DEG) bend up near the edges of the sample, forming edge states (ES) at the lines of intersection with the Fermi level. According to the picture of Büttiker,[1] transport in two-dimensional electron systems takes place mostly in ES because of a zero bulk dissipative conductivity in the quantum Hall effect regime. This single-particle picture was modified by Chklovskii *et al.*,[2] taking into account electrostatic interactions between electrons. This leads to the appearance of a set of incompressible and compressible strips near the 2DEG edge. This ES picture is nowadays widely accepted and is in good agreement with experimental results.[3]

Several experiments were performed, investigating not only transport along the 2DEG edge but also inter-edge-state charge transfer.[3] In charge transfer between the two spin-split ES of the lowest Landau level, the necessity for spin flips diminishes the tunneling probability. For this reason, the equilibration length between spin-split edge states can be as high as 1 mm at low temperatures, despite the large spatial overlap of electron wave functions.[4,5]

Formerly, the electron spin flip was attributed to spin-orbit coupling[5,6] while today it is known that the electron spin flip can be accompanied by the spin flop of a nucleus [the so-called dynamic nuclear polarization (DNP)] near the edge.[7–9] A key feature of this effect is a pronounced hysteresis of the *I-V* traces due to the high nuclear-spin-lattice relaxation time T_1, which was also reported for the bulk.[10–13] All experiments in which DNP was studied were prepared under condition of weak imbalance between edge channels.[7–9,14] On the other hand, new physical effects such as a hysteresis due to the switching of the positions of two ES (Ref. 15) are predicted in the regime of high imbalance.

Here we apply a quasi-Corbino geometry[16,17] to study electron transport between spin-resolved ES at chemical potential difference exceeding the spectral gap, i.e., at high imbalance. We find a pronounced hysteresis in the *I-V* curves, originating from slow relaxation processes, qualitatively different for positive and negative branches of *I-V* curve. Just in the simplest case of the filling factor $\nu=2$ we determine two characteristic relaxation times. All experimental observations are explained in the terms of the dynamic nuclear polarization via the hyperfine interaction.

II. SAMPLES AND EXPERIMENTAL TECHNIQUE

The samples are fabricated from two molecular-beam epitaxial-grown GaAs/AlGaAs heterostructures with different carrier concentrations and mobilities. One of them (*A*) contains a 2DEG located 70 nm below the surface. The mobility at 4 K is 800 000 $\mathrm{cm^2/V\,s}$ and the carrier density $3.7\times10^{11}\ \mathrm{cm}^{-2}$. For heterostructure *B* the corresponding parameters are 110 nm, $2.2\times10^{6}\ \mathrm{cm^2/V\,s}$, and $1.35\times10^{11}\ \mathrm{cm}^{-2}$. We obtain similar results on samples of both materials. For this reason we restrict the discussion here to results obtained from samples of wafer *A*.

Samples are patterned in a quasi-Corbino geometry[16] (see Fig. 1). The square-shaped mesa has a rectangular etched region inside. Ohmic contacts are made to the inner and outer edges of the mesa. The top gate does not completely encircle the inner etched region but leaves uncovered a narrow (3 μm) strip (gate gap) of 2DEG at the outer edge of the sample. The electron concentration in the gate-gap region (i.e., the positions of the filling factors in magnetic field) is determined from the oscillations of the two-point magnetoresistance. Using different pairs of ohmic contacts we confirm the homogeneity of the sample. To obtain the dependence of the electron concentration under the gate on the gate voltage we measure the capacitance between the gate and 2DEG as a function of the gate voltage in different magnetic fields.

In a quantizing magnetic field at integer filling factors (e.g., $\nu=2$, see Fig. 1) edge channels run along the etched edges of the sample. Depleting the 2DEG under the gate to a smaller integer filling factor (e.g., $g=1$, as shown in the figure) some channels ($\nu-g$) are reflected at the gate edge and redirected to the outer edge of the sample. In the gate-gap region, edge channels originating from different contacts run in parallel along the outer (etched) edge of the sample, on a distance determined by the gate-gap width. Thus, the applied geometry allows us to separately contact edge states

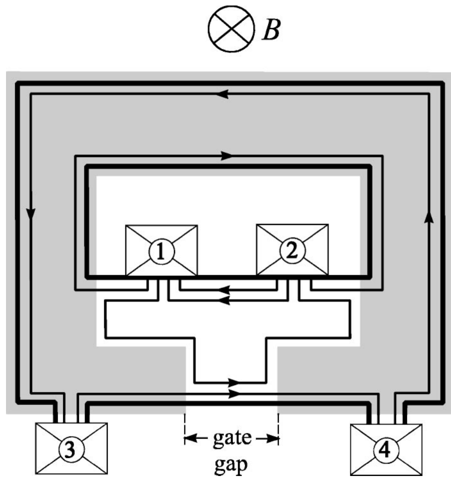

FIG. 1. Schematic diagram of the pseudo-Corbino geometry. Contacts are positioned along the etched edges of the ring-shaped mesa. The shaded area represents the Schottky gate. Arrows indicate the direction of electron drift in the edge channels for the outlined configuration: filling factors are $\nu = 2$ in the ungated regions and $g = 1$ under the gate.

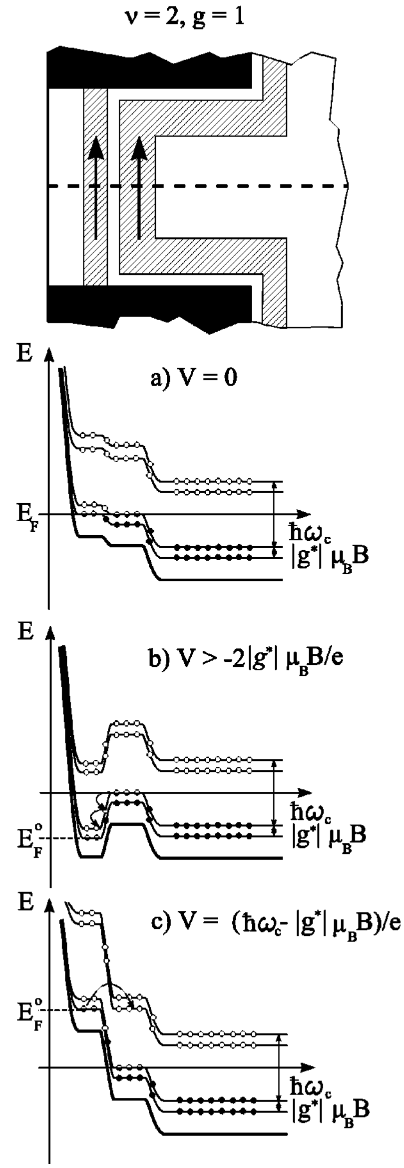

FIG. 2. Energy subband diagram of the sample edge in the gate gap for the filling factors $\nu = 2$ and $g = 1$. (a) No voltage V applied between inner and outer edge states. (b) $V > 0$, in the situation shown, the outer edge state is shifted down in energy by $eV < -2|g^*|\mu_B B$. (c) $V < 0$, here the energy shift $eV > 0$. Arrows in (b) and (c) show new ways for electron relaxation which become open at high imbalance.

and bring them into an interaction on a controllable length. A voltage applied between inner and outer ohmic contacts makes it possible to produce a significant imbalance between edge channels because the gate-gap width of a few microns is much smaller than the typical equilibration length between ES (more than 100 μm at low temperatures[3,5,16]).

In our experimental setup, a positive bias $V > 0$ shifts the outer ES down in energy with respect to the inner one [see Fig. 2(b)] (one inner ohmic contact is grounded, $e < 0$ is the electron charge). Therefore, at voltages close to the energy which separates the involved edge states, the potential barrier between edge states disappears and a significant current starts to flow.[7,16] In contrast, a negative bias steepens the potential relief [see Fig. 2(c)], so that electrons at any negative bias have to tunnel through the magnetic-field-induced barrier. Experimental I-V traces are expected to be nonlinear and asymmetric with a characteristic onset voltage on the positive branch, roughly equal to the corresponding energy gap (for a more thorough discussion see Ref. 16). A current in this case directly reflects a charge transfer between edge channels in the gate gap in contrast to the conventional Hall-bar geometry with crossing gates.[5] Whereas, no clear onset behavior can be seen for negative applied voltages.

Adjusting both, magnetic field B and gate voltage V_g, it is possible to change the number of ES in the gate-gap region (equal to the bulk filling factor ν) and—independently—the number g of ES transmitted under the gate. Thus the applied geometry allows us to study transport between spin-split or cyclotron-split edge channels depending on the adjusted filling factors ν and g.

We obtain I-V curves from dc four-point measurements at a temperature of 30 mK in magnetic fields up to 16 T. The measured voltages V are always much smaller than the gate voltage, so the electron density under the gate is unchanged during the I-V sweeps. The results presented in the paper are temperature independent below 0.5 K.

III. EXPERIMENTAL RESULTS

A typical I-V curve is shown in Fig 3(a) for the filling factor combination $\nu = 3$, $g = 2$ ($B = 5.2$ T, $V_g = -196$ mV). The I-V trace reflects transport in the gate gap between cyclotron-split edge states. It is strongly nonlinear and asymmetric with a positive onset voltage close to the value of the cyclotron energy.[16] The negative branch of the trace changes its slope at a voltage also comparable to $\hbar\omega_c/e$, due to the crossing of the outer (partially filled) ES with the excited (empty) level in the inner one.

Figure 3(b) shows an I-V curve for the filling factor combination $\nu = 3$, $g = 1$ ($B = 5.2$ T, $V_g = -372$ mV) which cor-

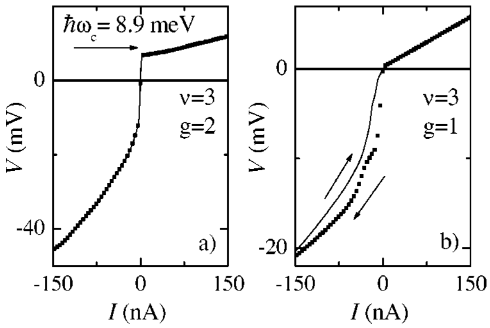

FIG. 3. I-V curves for filling factor combinations (a) $\nu=3$, $g=2$ (cyclotron splitting) and (b) $\nu=3$, $g=1$ (spin splitting). The solid line indicates a sweep from negative to positive currents and dots represent the reverse sweep direction. The arrow in (a) denotes the theoretical value of the cyclotron gap, whereas the arrows in (b) exhibit the sweep directions. For the dotted curves the number of points is reduced by ten times for reasons of clarity. The magnetic field is 5.2 T, the gate voltages are $V_g=-196$ mV for $\nu=3$, $g=2$ fillings and $V_g=-372$ mV for $\nu=3$, $g=1$ ones.

responds to transport between spin-split ES. The onset voltage on the positive branch is much smaller in this case, because of the smaller value of the spin gap in comparison to the cyclotron gap. However, the most important difference from Fig. 3(a) is a large hysteresis for the negative branch of the I-V curve.

The curves in Fig. 3 are obtained by continuous sweep from positive to negative currents and vice versa. Increasing the sweep rate increases the hysteresis effect. This indicates that the hysteresis is the result of a long-time relaxation process, in agreement with previous studies.[7,8] In our case a characteristic time is comparable to the sweep time of about ten min.

The described behavior is contrary to the one observed for transport through the cyclotron splitting [see Fig. 3(a)] where there is no hysteresis effect discernible. Because of the much smaller bulk 2DEG dissipative conductivity under the gate for cyclotron split filling factors, this shows that the hysteresis for $\nu=3$, $g=1$ cannot be caused by the charging of the bulk 2DEG. This fact was checked for different filling factor combinations on samples from two different wafers: the hysteresis is present only for transport between spin-split edge channels and there is no hysteresis in the I-V curves corresponding to cyclotron splitting.

We investigate in more detail the simplest filling factor combination $\nu=2, g=1$ ($B=7.7$ T, $V_g=-288$ mV) for which only two ES take part in an equilibration process. The zero-bias region of the I-V trace for this filling factor combination is shown in Fig. 4 to demonstrate that hysteresis is also observable for the positive branch. The asymmetry of the I-V curve is also reflected in the hysteresis: at negative biases it is more pronounced, while for positive branch hysteresis it is observable at relatively small currents only.

To directly investigate the time dependence of the relaxation, we measure the change of the voltage drop at different fixed currents. To prepare a stable state of the system, a

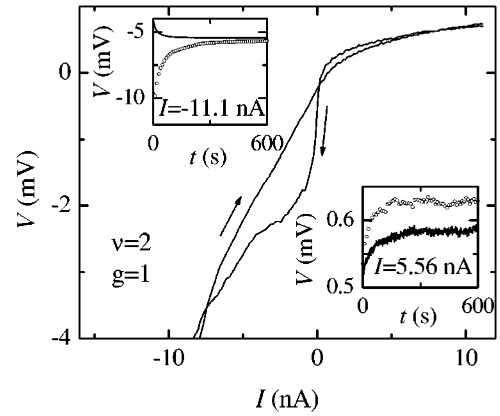

FIG. 4. I-V curves for the filling factor combination $\nu=2$, $g=1$ (spin splitting) for small biases. The two different sweep directions are indicated by arrows. Insets show the relaxation curves at fixed currents $I=-11.1$ nA (left inset) and $I=5.56$ nA (right inset) obtained for two dwelling currents $I^-_{dwell}=-222$ nA (solid curves) and $I^+_{dwell}=111$ nA (dotted ones). The magnetic field is 7.7 T, the gate voltage $V_g=-288$ mV.

dwelling current I_{dwell} is applied for a time long enough (about 10 min) to observe a stable voltage drop. This procedure provides a reproducible initial state of the system. Directly switching to a current I after the dwell, we measure the time-dependent voltage drop $V(t)$. The resulting $V(t)$ curves are well reproducible.

Examples of these $V(t)$ dependencies are shown in the insets of Fig. 4. For both, positive and negative branches of the I-V trace, time-dependent relaxation is measured after dwelling at two different currents $I^+_{dwell}=111$ nA (circles) and $I^-_{dwell}=-222$ nA (solid curves). We stress that both branches of the I-V traces differ not only in the size of the relaxation (by two orders of magnitude) but also in the dependence on the sign of the dwelling current. For the positive branch ($I>0$) $V(t)$ curves are qualitatively independent of the sign of I_{dwell} and the relaxation always appears as an increase in the resistance. For the negative branch ($I<0$), on the other hand, the resistance is increasing with time for negative $I^-_{dwell}<0$ and decreasing for a positive one $I^+_{dwell}>0$. Thus, for the negative branch of the I-V trace the character of the relaxation as well as its starting value are very sensitive to the sign of I_{dwell}.

The experimental $V(t)$ curves seem to obey an exponential law of relaxation but clearly consist of two different regions. We find that the relaxation curves for transport between two spin-split edge channels at negative currents can well be fitted by a double-exponential decay,

$$V(t)=V_0+V_1\exp\left(-\frac{t}{\tau_1}\right)+V_2\exp\left(-\frac{t}{\tau_2}\right), \qquad (1)$$

as shown in Fig. 5 (solid curve). For a comparison, a single-exponential fit (dashed curve in Fig. 5) is given, which cannot describe adequately the experimental data, especially for $t>50$ s. The inset in semilogarithmic axes demonstrates

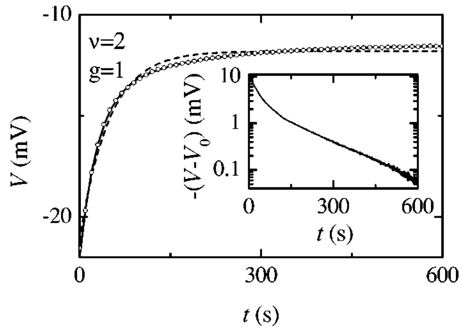

FIG. 5. Relaxation curve for the filling factor combination $\nu = 2$, $g = 1$ at $I = -22.2$ nA for a positive dwelling current $I^{+}_{dwell} = 111$ nA (circles). The number of points is diminished by ten times for clarity. The solid curve indicates a fit by a double-exponential decay function [Eq. (1)], the dashed one is a fit by one exponential function only. The inset shows the same experimental relaxation curve in a semilogarithmic plot shifted by $V_0 = V(t = \infty) = -11.5$ mV.

clearly the presence of the second exponential dependence which especially dominates the long-time behavior.

The decay times obtained from the double-exponential fit are shown as a function of current in Fig. 6. The times are practically independent of the dwelling current, but slowly dependent on cooling procedure. The maxima in the $\tau(I)$ dependence are qualitatively reproducible from cooling to cooling and from sample to sample. For positive currents (positive branch of the I-V trace) the accuracy of the determination of τ_2 is smaller than for negative ones because of the smaller value of the relaxation (see inset to Fig. 4), nevertheless both times have the same order of magnitude for both branches. Measurements of the relaxation in tilted fields show that the time constants τ_1 and τ_2 [and the maxima position in $\tau(I)$ dependence] are also independent of the in-plane magnetic field.

From the $V(t)$ curves the time-independent, steady state of the system can be extrapolated. It can be obtained either from V_0 as a fitting parameter [see Eq. (1)] or as the last value of the relaxation curve at $t = 600$ s. The difference is negligible. The resulting steady-state I-V traces are presented in Fig. 7 for normal and tilted magnetic fields. It

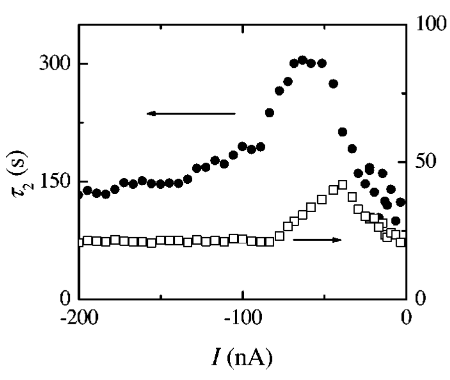

FIG. 6. Relaxation times τ_1 (squares) and τ_2 (circles) for the filling factor combination $\nu = 2$, $g = 1$ for a positive dwelling current $I^{+}_{dwell} = 111$ nA.

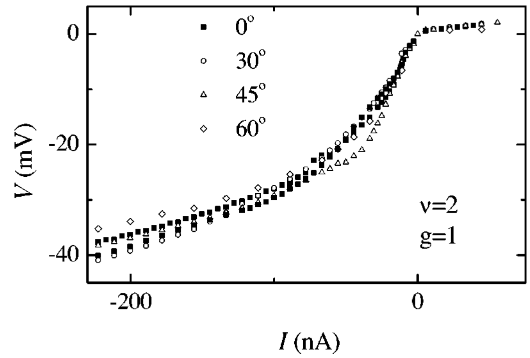

FIG. 7. Steady-state I-V curves for normal and tilted magnetic fields for filling factors $\nu = 2$, $g = 1$. The tilt angles shown are 0°, 30°, 45°, and 60°. At normal magnetic field the results of two different cooling cycles of the sample are presented.

can be seen that the stationary I-V curves are independent with experimental accuracy of the in-plane component of the magnetic field. The deviations are of the same order as the difference between two different cooling cycles at zero tilt angle.

For other spin-split filling factor combinations (such as $\nu = 3$, $g = 1$) a larger number of edge channels is involved in the transport. Besides charge transfer among spin-split ES in the gate gap, cyclotron-split edge channels have to be taken into account. As a result, the relaxation process is more complicated and it is found in the experiment that the resistance is no longer a monotonic function of time. Some influence of the in-plane magnetic field on the steady-state I-V traces is observable for these filling factor combinations. The resistance on the negative branch decreases with increasing in-plane magnetic field because of the reduction of the cyclotron gap.[18]

IV. DISCUSSION

For electron transfer between spin-resolved ES it is necessary to change both the spin and the spatial position of the electron. For this reason, we consider three possible mechanisms for the electron transfer: (i) magnetic impurities, (ii) spin-orbit interaction, and (iii) hyperfine interaction. An influence of the magnetic impurities can be excluded because of the high quality of the MBE process for GaAs/AlGaAs, taking into account the fact that our samples, which are grown in two different MBE systems, exhibit similar behavior.

The spin-orbit interaction is well known to be responsible for electron transfer between ES at small imbalance.[5,6] It will be shown below that the main part of interedge current on the left I-V branch in our samples flows between ES in this way. However, spin-orbit coupling cannot explain a voltage relaxation on the macroscopic time scale of the order of $\tau_1 \sim 25$ s. On the other hand, the obtained relaxation time $\tau_1 \sim 25$ s is close to the nuclear-spin-relaxation times in GaAs (of the order of 30 s, Refs. 7 and 8). For this reason, the relaxation of I-V curves should be attributed, in agreement with Refs. 7–9, to the hyperfine interaction.

A Hamiltonian of the hyperfine interaction can be written as

$$A\boldsymbol{I}\cdot\boldsymbol{S}=\tfrac{1}{2}(I^{+}S^{-}+I^{-}S^{+})+AS_zI_z\,, \tag{2}$$

where $A>0$ is the hyperfine constant, $\boldsymbol{I}$ is the nuclear spin, and $\boldsymbol{S}$ is the electron spin.

At the temperature of the experiment (30 mK) in a magnetic field (below 16 T) the static nuclear polarization $\langle I_z\rangle$ by the external magnetic field is negligible. Nevertheless, a significant *dynamic* polarization of the nuclei is possible: an electron spin-flip causes the spin flop of a nucleus in the GaAs lattice as described by the first term in Eq. 2 (the so-called flip-flop process). Thus a part of the current flow between spin-resolved edge channels produces a DNP $\langle I_z\rangle$ in the edge region of the sample.[7,8] This polarization affects the electron energy through the second term in Eq. (2) (the Overhauser shift), which leads to the change of I-V curve. The influence of the nuclear polarization on the electron energy can be conveniently described by the effective Overhauser field $B_{Ov}=A\langle I_z\rangle/g^*\mu_B$ which affects the Zeeman splitting $|g^*|\mu_B(B+B_{Ov})$.

The relaxation behavior for both positive and negative currents can be interpreted in terms of DNP, despite the strong difference in relaxation on the left and right branches of the I-V curve. Because of the negative effective g factor ($g^*=-0.44$ in bulk GaAs), electron spins in the outer ES are polarized in the field direction (''up polarization'') while in the inner ES they are polarized ''down.''

(i) A negative applied bias shifts the outer ES up in energy with respect to the inner one [see Fig. 2(c)]. Electrons tunnel through the incompressible strip between outer and inner ES with a spin flip from up to down. Some of these electrons relax due to the spin-orbit coupling, changing their energy by phonon emission. Nevertheless, the transitions from filled to empty states across incompressible strip are also possible due to the flip-flop process. Electron energy in this process remains practically unchanged. The electron spin-flip from up to down leads to a nuclear spin flop from down to up. Thus, a current persisting for a long time induces in the gate gap a DNP with $\langle I_z\rangle>0$. Because of the negative g^* factor in GaAs, the effective Overhauser field is antiparallel to the external field $B_{Ov}<0$ and decreases the value of the Zeeman splitting $|g^*|\mu_B(B+B_{Ov})$.

(ii) For a positive bias exceeding the onset voltage $V_{on}\sim-|g^*|\mu B/e$, there is no more potential barrier for electrons between edge states [see Fig. 2(b)]. Electrons flow from the inner to the outer ES and rotate the spin in vertical transitions afterwards (e.g., by emitting a photon), possibly far from the gate-gap region. Nevertheless, for a bias $V>2V_{on}$ electrons can also tunnel from the filled (spin up) state to the empty one (spin down) in the incompressible strip due to the flip-flop mechanism, relaxing later to the ground state vertically. This flip flop also produces an up nuclear polarization $\langle I_z\rangle>0$ in the gate-gap accompanied by an Overhauser field $B_{Ov}<0$ antiparallel to the external magnetic field, which diminishes the Zeeman splitting.

The value of the net nuclear polarization $\langle I_z\rangle$ is therefore determined by the current connected with flip-flop processes which in turn is controlled by the applied bias V [see Fig. 2(c)]. Thus, after dwelling at a positive current and switching to a negative one the nuclear polarization (i.e., the Overhauser field) increases significantly during the relaxation process, diminishing the Zeeman splitting. As the Zeeman splitting determines the spatial distance between spin-split ES, the tunneling length for the electrons decreases during the relaxation process.[8] For this reason, in the described situation, the relaxation goes along with a decrease of the resistance, as seen in the experiment [left inset of Fig. 4 (dots)].

Dwelling at a high negative current and switching to a lower one (i.e., closer to the zero), the nuclear polarization diminishes in value. The corresponding change in the Overhauser field increases the Zeeman splitting. As a result, the tunneling length is rising, leading to an increase of the resistance, as depicted by the solid curve in the left inset to Fig. 4.

After a dwell at a negative or large positive current and switching to a small positive one, the nuclear polarization is always diminishing in value, leading to an increase of the resistance, as can be seen in the right inset to Fig. 4.

The presence of the two different relaxation times in the experimental traces can result directly from the injection of spin-polarized electrons in the gate-gap region of the applied experimental geometry (Fig. 2, for a model calculation of a similar problem see Ref. 19). The characteristic time scale for establishing the Overhauser field in the gate gap is governed by the applied current and the diffusion of the nuclear polarization from the gate-gap region because of nuclear spin-spin interactions. A combination of these two processes should be responsible for the first relaxation with the characteristic time $\tau_1\sim25$ s. However, diffusion takes place on length scales much larger than the gate-gap width but smaller than the sample size. The second relaxation process with the characteristic time τ_2 of the order of the nuclear spin-lattice relaxation time T_1 is therefore attributed to the establishing of a stable nuclear polarization outside the gate gap. The origin of the maxima in $\tau(I)$ dependencies is still unclear for us. The fact that both times are a maximum simultaneously gives a strong evidence that the observed time increase is not an artifact. The maxima are also reproducible from cooling to cooling and from sample to sample and practically independent of the in-plane magnetic field. As for other spin-split filling factor combinations, because of larger number of the edge channels involved into the charge transfer, the relaxation process is more complicated and it is difficult to quantitatively analyze the relaxation times.

Assuming the lattice period in GaAs to be 5.6 Å with two atoms per unit we can estimate the full number of nuclei in the gate gap to be $2\times3\ \mu\text{m}\times200\ \text{Å}\times1000\ \text{Å}/(5.6\ \text{Å})^3\sim10^8$. In the stationary regime the gate gap is highly polarized, i.e., the number of the polarized nuclei N_{pol} is about the full number of nuclei in the gate gap. The part of the current connected with flip-flop processes is given by N_{pol} and the first relaxation time $I_N\sim eN_{pol}/\tau_1\sim10^{-13}$ A. It means that for a current of about 1 nA between ES only one electron out of 10 000 will flip a nuclear spin.

V. CONCLUSION

Performing direct measurements of the electron transport between spin-split edge states at high imbalance, we found a long-time relaxation which is absent for charge transfer between cyclotron-split edge states. The characteristic times are of the order of 25 s and 200 s, which points to the presence of two different relaxation mechanisms. We attribute this relaxation to the formation of a DNP near the sample edge. The presence of the two relaxation mechanisms is interpreted as the formation of a DNP inside the gate-gap region due to flip-flop processes and outside it as a consequence of the diffusion of nuclear spins. We also found that an in-plane magnetic field has no influence both on the relaxation between two spin-split edge channels and on the steady state of the system.

ACKNOWLEDGMENTS

We wish to thank Dr. A. A. Shashkin for help during the experiments and discussions. We gratefully acknowledge financial support by the Deutsche Forschungsgemeinschaft, SPP ''Quantum Hall Systems,'' under Grant No. LO 705/1-2. The part of the work performed in Russia was supported by RFBR, and the programs ''Nanostructures'' and ''Mesoscopics'' from the Russian Ministry of Sciences. V.T.D. acknowledges support by A. von Humboldt foundation.

*Corresponding author. Email address: dev@issp.ac.ru

[1] M. Büttiker, Phys. Rev. B **38**, 9375 (1988).
[2] D.B. Chklovskii, B.I. Shklovskii, and L.I. Glazman, Phys. Rev. B **46**, 4026 (1992).
[3] For a review, see R.J. Haug, Semicond. Sci. Technol. **8**, 131 (1993).
[4] A.A. Shashkin, V.T. Dolgopolov, G.M. Gusev, and Z.D. Kvon, JETP Lett. **53**, 461 (1991).
[5] G. Müller, D. Weiss, A.V. Khaetskii, K. von Klitzing, S. Koch, H. Nickel, W. Schlapp, and R. Lösch, Phys. Rev. B **45**, 3932 (1992).
[6] A.V. Khaetskii, Phys. Rev. B **45**, 13 777 (1992).
[7] David C. Dixon, Keith R. Wald, Paul L. McEuen, and M.R. Melloch, Phys. Rev. B **56**, 4743 (1997).
[8] T. Machida, S. Ishizuka, T. Yamazaki, S. Komiyama, K. Muraki, and Y. Hirayama, Phys. Rev. B **65**, 233304 (2002).
[9] Tomoki Machida, Tomoyuki Yamazaki, and Susumu Komiyama, Appl. Phys. Lett. **80**, 4178 (2002).
[10] M. Dobers, K.v. Klitzing, J. Schneider, G. Weimann, and K. Ploog, Phys. Rev. Lett. **61**, 1650 (1988).
[11] A. Berg, M. Dobers, R.R. Gerhardts, and K.v. Klitzing, Phys. Rev. Lett. **64**, 2563 (1990).
[12] B.E. Kane, L.N. Pfeiffer, and K.W. West, Phys. Rev. B **46**, 7264 (1992).
[13] W. Desrat, D.K. Maude, M. Potemski, J.C. Portal, Z.R. Wasilewski, and G. Hill, Phys. Rev. Lett. **88**, 256807 (2002).
[14] R.J. Haug, A.H. MacDonald, P. Streda, and K. von Klitzing, Phys. Rev. Lett. **61**, 2797 (1988).
[15] Lex Rijkels and Gerrit E.W. Bauer, Phys. Rev. B **50**, 8629 (1994).
[16] A. Würtz, R. Wildfeuer, A. Lorke, E.V. Deviatov, and V.T. Dolgopolov, Phys. Rev. B **65**, 075303 (2002).
[17] G. Müller, E. Diessel, D. Wiess, K. von Klitzing, K. Ploog, H. Nickel, W. Schlapp, and R. Lösch, Surf. Sci. **263**, 280 (1992).
[18] J.J. Koning, R.J. Haug, H. Sigg, K. von Klitzing, and G. Weimann, Phys. Rev. B **42**, 2951 (1990). Our measurements of the onset voltage for the positive branch at cyclotron split filling factor combinations will be published elsewhere.
[19] Yu.V. Pershin, S.N. Shevchenko, I.D. Vagner, and P. Wyder, Phys. Rev. B **66**, 035303 (2002).